AJNR

Three-Dimensional Fusion Digital Subtraction Angiography: New Reconstruction Algorithm for Simultaneous Three-Dimensional Rendering of Osseous and Vascular Information Obtained during Rotational Angiography

Philippe Gailloud, Satoru Oishi and Kieran Murphy

AJNR Am J Neuroradiol 2005, 26 (4) 908-911
http://www.ajnr.org/content/26/4/908

Three-Dimensional Fusion Digital Subtraction Angiography: New Reconstruction Algorithm for Simultaneous Three-Dimensional Rendering of Osseous and Vascular Information Obtained during Rotational Angiography

Philippe Gailloud, Satoru Oishi, and Kieran Murphy

Summary: This report describes three-dimensional (3D) fusion digital subtraction angiography (FDSA), a new algorithm for rotational angiography that combines reconstructions of the blood vessels and the osseous frame in a single 3D representation. 3D-FDSA is based on separate reconstructions of the mask and contrast sequences of the rotational acquisition. The two independent 3D data sets (3D-bone and 3D–digital subtraction angiography [DSA]) are fused in a single 3D representation. The algorithm uses a modification of the Feldkamp method that compensates for signal intensity inhomogeneity inherent to the reconstruction of nonsubtracted rotational acquisitions. By separately reconstructing the osseous and vascular information obtained from the rotational angiogram, 3D-FDSA provides optimal angiographic resolution and precise topographic analysis even when the studied vascular tree is in the immediate vicinity of bone.

Digital subtraction angiography (DSA) remains the most accurate imaging technique for the evaluation of the cerebrovascular system (1). The newly developed technique of three-dimensional (3D)–DSA has even further enhanced the accuracy of DSA for the diagnosis of intracranial vascular anomalies (2–5). However, noninvasive imaging techniques, such as MR angiography and CT angiography, have also shown remarkable progress. In particular, CT angiography is a promising technique for the diagnosis of intracranial vascular lesions, such as cerebral aneurysms. Furthermore, CT angiography provides simultaneous 3D rendering of vascular structures and their osseous environment, an option previously not available with conventional angiographic techniques (1, 6, 7). 3D–digital angiography (DA), a newly introduced reconstruction algorithm for rotational conventional angiography, now offers concomitant high-resolution representation of bone and blood vessels (8). However, because the algorithm for 3D-DA is based on the reconstruction of a single, nonsubtracted rotational data set, it cannot avoid an artifactual loss of image quality when osseous and vascular structures are immediately adjacent (8). This problem, which typically affects the imaging of vascular lesions located at the skull base, is common to both 3D-DA and CT angiography (6).

The present technical report describes 3D–fusion DSA (FDSA), a new algorithm for rotational angiography that combines separate reconstructions of the blood vessels and the osseous frame in a single 3D representation. The technique is illustrated by a clinical example involving the analysis of vascular structures at the skull base.

Technique

Data Acquisition

3D-FDSA is performed by applying a new reconstruction algorithm to standard rotational cerebral angiography. The parameters used for rotational angiography with our equipment (Infinix NB, Toshiba, Japan) are as follows: tube rotation −200° at 40°/seconds, frame rate −30 frames per second. A nonionic iodinated contrast agent (Omnipaque 300; Amersham Health, Princeton, NJ) is administered with an automatic injector by using a typical volume and rate of 24 mL and 4 mL/second, respectively, for the common carotid artery and 18 mL and 3 mL/second, respectively, for the vertebral artery.

3D Image Postprocessing

3D-FDSA images are generated from the same rotational data set used for standard 3D-DSA reconstruction. To obtain 3D-FDSA images, the two components of the rotational acquisition, ie, the series of mask images and the series of contrast images, have to go through a three-step reconstruction process (Fig 1):

Step 1 is the 3D reconstruction of the vascular tree of interest; it is equivalent to a standard 3D-DSA technique. First, a rotational DSA data set is built by subtracting angle-matched mask images from the contrast images. The 3D representation of the vascular tree is then reconstructed from the subtracted rotational images by using the Feldkamp method (8).

Step 2 consists in the independent reconstruction of a 3D

Received April 26, 2004; accepted after revision September 8.

From the Division of Interventional Neuroradiology, the John Hopkins Hospital, Baltimore, MD (P.G., K.M.), and Toshiba Medical Systems, Research and Development Center, Tochigi, Japan (S.O.).

Address reprint requests to Philippe Gailloud, MD, Division of Interventional Neuroradiology, Russell H. Morgan Department of Radiology and Radiological Sciences, the John Hopkins Hospital, Nelson B-100, 600 N Wolfe St, Baltimore, MD 21287.

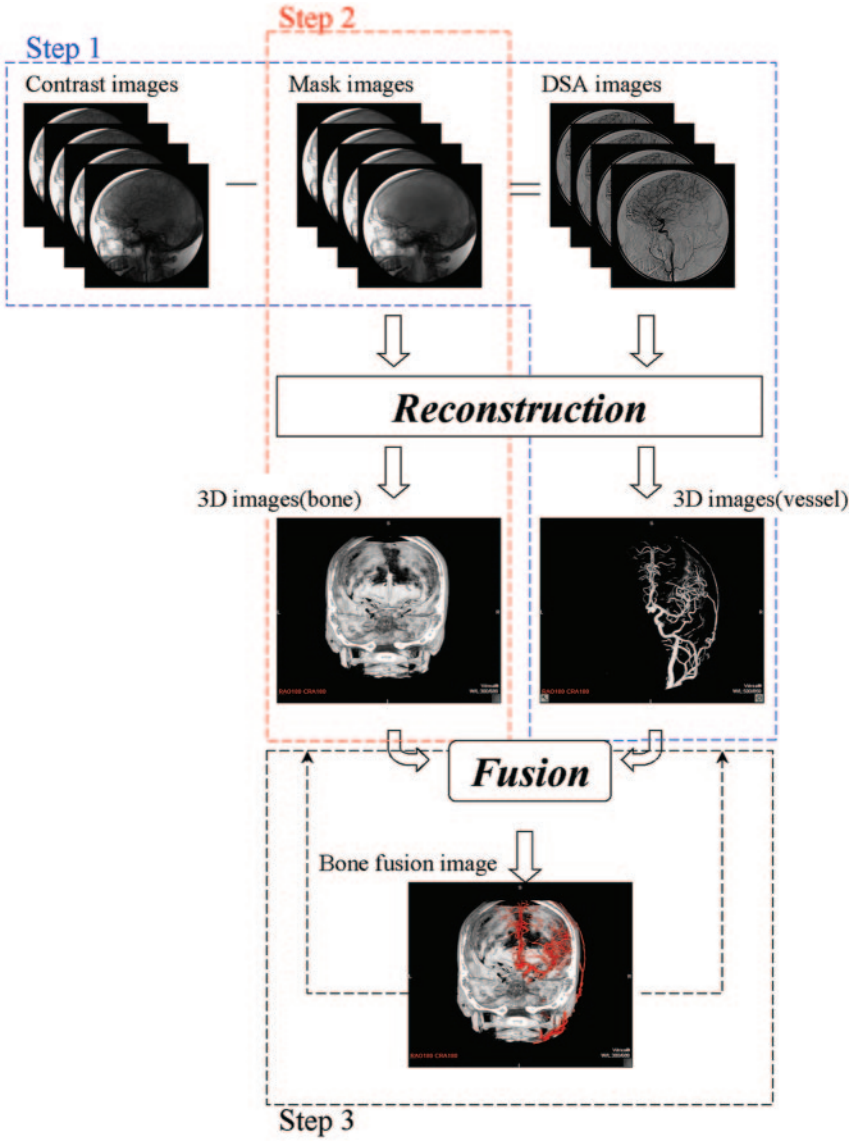

FIG 1. Flowchart shows the three steps involved in 3D-FDSA image reconstruction. The first (outlined in *blue*) consists in a standard 3D-DSA reconstruction. The rotational mask acquisition is subtracted from the rotational contrast acquisition. The Feldkamp method is applied to the resulting subtracted rotational data set to obtain the 3D-DSA reconstruction. The second step (outlined in *red*) consists in the reconstruction of the rotational mask acquisition into a 3D osseous representation (3D-bone) by using a modified Feldkamp method. The third step (outlined in *black*) is the combination of the two 3D reconstructions obtained in step 1 and 2 into a fused 3D volume.

image of the osseous frame (3D-bone) from the rotational mask acquisition used in step 1. The nonuniformity of brightness inherent to the imaging chain is compensated by subtracting a flood image from each mask image. The flood image is acquired without phantom as part of a monthly calibration process. The 3D-bone representation is reconstructed from the compensated mask images by using a modified Feldkamp method (8).

Step 3 builds the 3D-FDSA representation by fusing the 3D-DSA and 3D-bone data sets obtained through steps 1 and 2. Because the 3D-DSA and 3D-bone representations share an identical coordinate system, they can be fused in a single 3D space without additional registration operations. A volume-rendering technique is then applied to the fused 3D data set (3D-FDSA). Different color settings are applied to the vascular and osseous components of the 3D image during the volume-rendering process to enhance structure differentiation and recognition.

The postprocessing workstation offers three 3D display modes of a single rotational data set: 3D-FDSA, 3D-DSA, and 3D-bone. Switching from one mode to the other is instantaneous by means of a mouse click. The 3D volume can be trimmed or a volume-of-interest can be created by using free-drawing tools to focus the 3D representation on a specific region of interest. The 3D data set can also be reformatted in various two-dimensional (2D) representations (standard orthogonal, oblique, or curved) of various section thicknesses.

Case Illustration

A 32-year-old neurologically intact woman was examined for tinnitus. MR imaging depicted a vascular mass centered in the left petrous region, and she was referred to our institution for further investigation. 3D-FDSA was performed during routine conventional angiography. DSA revealed a large fusiform aneurysm in the distal left internal carotid artery. The 3D-FDSA images emphasized the relation of the mass with the surrounding structures, revealing in particular a protrusion of the aneurysmal sac into the posterior fossa through an adjacent bony erosion (Fig 2). Therapeutic sacrifice of the left internal carotid artery with coils and detachable balloons was performed after an uneventful balloon-occlusion test.

Discussion

Introduced in 1927 by Egas Moniz and Almeida Lima, cerebral angiography was immediately considered a potential breakthrough for the diagnosis of intracranial pathologies (9). The development of safe

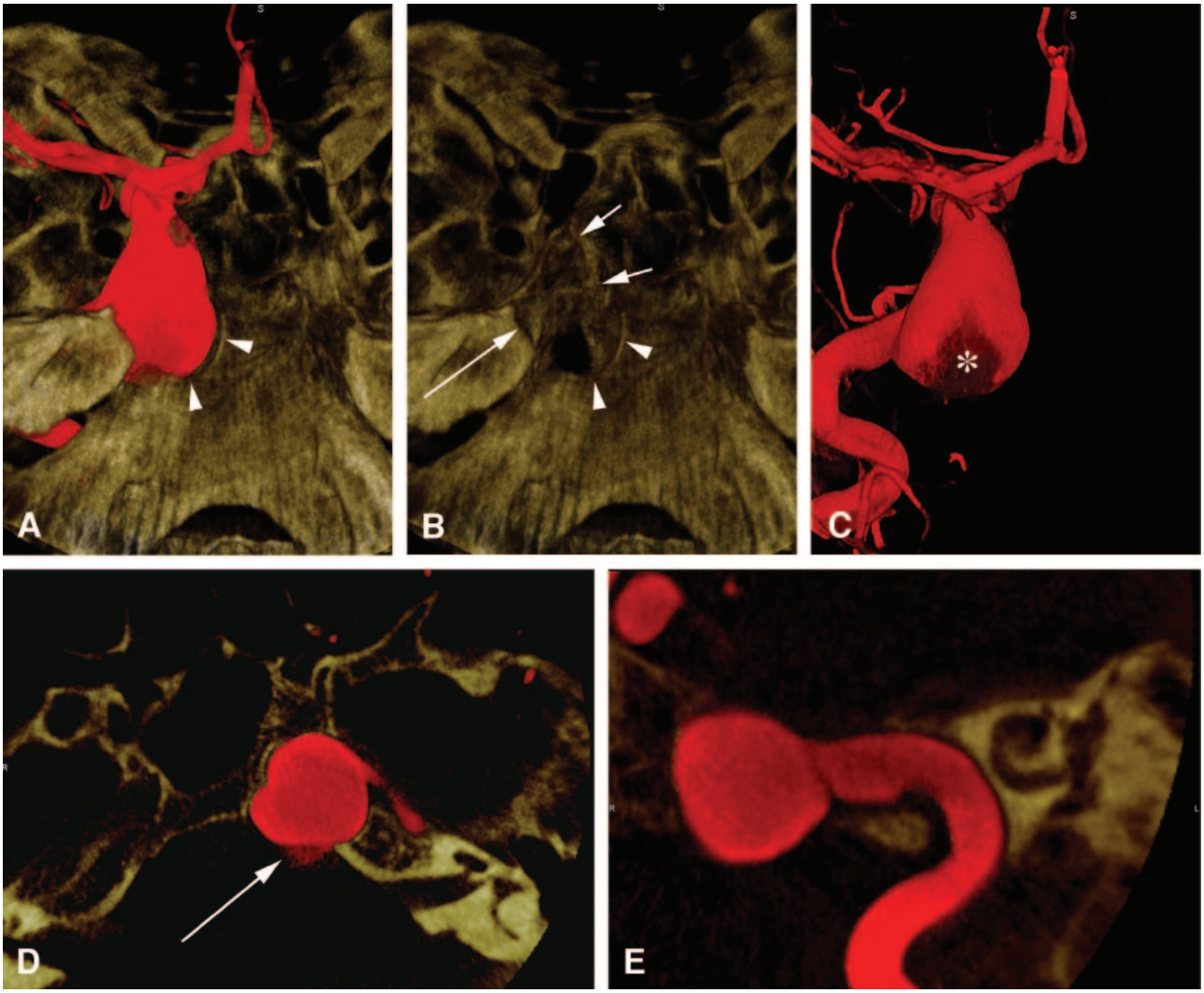

FIG 2. 3D-FDSA a 32-year-old woman with a fusiform aneurysm of the left internal carotid artery. Representations on the workstation include 3D-FDSA, 3D-bone, and 3D-DSA modes.

A, Craniocaudal 3D-FDSA view of the skull base shows erosion of the basisphenoid due to expansion of the aneurysm (*arrowheads*).

B, Same view in 3D-bone mode better depicts the osseous erosion involving the basisphenoid (*arrowheads*), apex of the petrous bone (*long arrow*), and lateral aspect of the sphenoid body (*short arrows*).

C, Same view in 3D-DSA mode provides details of the vascular anatomy. Note decreased attenuation in the posterior aspect of the aneurysm (*asterisk*) corresponding to the stagnation of contrast agent in the declive portion of the sac, as seen on regular 2D-DSA (not shown).

D, 2D axial reformation of the 3D-FDSA data set (section thickness, 1 mm) reveals that the posterior aspect of the aneurysmal cavity, where contrast agent stagnation is shown, protrudes into the posterior fossa through the eroded basisphenoid (*arrow*).

E, 2D reformation of the 3D-FDSA data set (section thickness, 1 mm) in an oblique plane parallel to the axis of the petrous bone. Note the detailed rendering of the interface between bone and blood vessels as the carotid artery crosses the carotid canal. Also note the fine anatomic depiction of the inner ear structures.

contrast agents, as well as the introduction of photographic and later electronic subtraction techniques (10–12), established modern cerebral DSA. Noninvasive cerebral imaging appeared in the late 1970s, with the introduction of CT and the subsequent advent of MR imaging. These techniques enabled direct visualization of the cerebral parenchyma for the first time and quickly superseded cerebral angiography in the evaluation of nonvascular intracranial lesions. More recently, noninvasive vascular-imaging techniques, such as CT and MR angiography as well as Doppler sonography, have been used in place of DSA for the diagnosis of certain neurovascular conditions, including extracranial carotid artery disease. Despite these advances, DSA remains the criterion standard imaging technique for the evaluation of the cerebral vasculature (1). 3D-DSA, which consists of the 3D reconstruction of a rotational angiographic data set, is the latest refinement in catheter-based angiographic techniques. 3D-DSA combines the anatomic resolution of DSA with 3D-rendering techniques previously available with only CT or MR angiography. 3D-DSA provides information more detailed than that of DSA alone in the evaluation of neurovascular lesions, such as cerebral aneurysms (2–5). This technique has taken a prominent role in treatment planning, as it improves

appreciation of the morphology of complex vascular lesions before endovascular or surgical management is undertaken. It is also superior in the performance of sophisticated tasks, such as measuring the volume of aneurysms (13). However, the inability of 3D-DSA to simultaneously depict osseous and vascular information is a weakness of the technique when compared with CT angiography (1, 6, 7).

A new reconstruction algorithm for rotational angiography that combines vascular and osseous information has been described (8). This new technique, termed 3D-DA, consists of the 3D reconstruction of a single, nonsubtracted rotational data set. Therefore, it offers simultaneous imaging of bone and blood vessels. However, the single-step reconstruction process, which is based on the analysis of differences in attenuation between opacified blood vessels and surrounding osseous structures, loses its accuracy when bone and vessels are immediately adjacent. This problem is similar to the limitations encountered during CT angiography at the skull base. The purpose of the reconstruction algorithm (3D-FDSA) that we present is to optimize simultaneous 3D rendering of osseous and vascular structures, particularly when these structures are contiguous, as in the skull base. To reach this goal, 3D-FDSA uses independent reconstructions of a subtracted rotational data set (equivalent to 3D-DSA) and of a nonsubtracted, noncontrast rotational data set (3D-bone), which is in fact derived from the mask images obtained as part of the 3D-DSA process. 3D-FDSA images are produced by fusing 3D-DSA and 3D-bone in a single 3D reconstruction.

3D-FDSA offers osseous and vascular information finer than that of 3D-DA for two reasons: First, 3D-DA images distinguish vascular and osseous structures by using thresholding techniques. However, the distributions of voxel attenuation values for bone and vessels overlap; therefore, these structures may be incorrectly recognized in the thresholding technique. With 3D-FDSA, the vascular and osseous volumes are separately reconstructed from individual rotational data sets, without additional manipulation such as thresholding. Second, the separate reconstruction process used for 3D-FDSA also avoids the summation of bone-related, beam-hardening artifacts and vascular artifacts (pulsatile structures, incomplete vessel opacification). These artifacts are superimposed in the one-step reconstruction of 3D-DA and degrade the fine anatomic detail.

The clinical case in which precise topographic analysis of the relationships between osseous and vascular structures was critical to both diagnosis and management illustrates the potential clinical applications of 3D-FDSA. In this case, 3D-FDSA depicted the bony erosion produced by the pulsating mass and revealed the aneurysmal sac bulging into the posterior fossa, which prompted therapeutic sacrifice of the carotid artery.

Conclusion

The combination of high-resolution vascular and bone imaging offered by 3D-FDSA further refines the role of conventional angiographic techniques in the diagnosis of cranial vascular lesions, particularly those located at the skull base. In addition, the fine anatomic and topographic information that 3D-FDSA provides can help optimize the planning of surgical or endovascular approaches to cerebrovascular diseases.

References

1. Chappell ET, Moure FC, Good MC. **Comparison of computed tomographic angiography with digital subtraction angiography in the diagnosis of cerebral aneurysms: a meta-analysis.** *Neurosurgery* 2003;52:624–631
2. Hochmuth A, Spetzger U, Schumacher M. **Comparison of three-dimensional rotational angiography with digital subtraction angiography in the assessment of ruptured cerebral aneurysms.** *AJNR Am J Neuroradiol* 2002;23:1199–1205
3. Hirai T, Korogi Y, Suginohara K, et al. **Clinical usefulness of unsubtracted 3D digital angiography compared with rotational digital angiography in the pretreatment evaluation of intracranial aneurysms.** *AJNR Am J Neuroradiol* 2003;24:1067–1074
4. Sugahara T, Korogi Y, Nakashima K, Hamatake S, Honda S, Takahashi M. **Comparison of 2D and 3D digital subtraction angiography in evaluation of intracranial aneurysms.** *AJNR Am J Neuroradiol* 2002;23:1545–1552
5. Abe T, Hirohata M, Tanaka N, et al. **Clinical benefits of rotational 3D angiography in endovascular treatment of ruptured cerebral aneurysm.** *AJNR Am J Neuroradiol* 2002;23:686–688
6. Hirai T, Korogi Y, Ono K, et al. **Preoperative evaluation of intracranial aneurysms: usefulness of intraarterial 3D CT angiography and conventional angiography with a combined unit–initial experience.** *Radiology* 2001;220:499–505
7. Nishihara M, Tamaki N. **Usefulness of volume-rendered three-dimensional computed tomographic angiography for surgical planning in treating unruptured paraclinoid internal carotid artery aneurysms.** *Kobe J Med Sci* 2001;47:221–230
8. Gailloud P, Oishi S, Carpenter J, Murphy KJ. **Three-dimensional digital angiography: new tool for simultaneous three-dimensional rendering of vascular and osseous information during rotational angiography.** *AJNR Am J Neuroradiol* 2004;25:571–573
9. Veiga-Pires JA, Grainger RG. *Pioneers in Angiography. The Portuguese School of Angiography.* Lancaster: MTP, 1982
10. Ziedses des Plantes BG. **Application of the roentgenographic subtraction method in neuroradiography.** *Acad Radiol* 1963;1:961–966
11. Ovitt TW, Christenson PC, Fisher HD III, et al. **Intravenous angiography using digital video subtraction: x-ray imaging system.** *AJR Am J Roentgenol* 1980;135:1141–1144
12. Mistretta CA, Crummy AB, Strother CM. **Digital angiography: a perspective.** *Radiology* 1981;139:273–276
13. Piotin M, Gailloud P, Bidaut L, et al. **CT angiography, MR angiography and rotational digital subtraction angiography for volumetric assessment of intracranial aneurysms: an experimental study.** *Neuroradiology* 2003;45:404–409